Electronic Supplementary Information

Phosphatase mimicking activity of a unique penta-nuclear zinc(II) complex with a reduced Schiff base ligand: Assessment of its ability to sense nitroaromatics

Mainak Karmakar, Tanmoy Basak, Shouvik Chattopadhyay*

Hirshfeld surfaces

Hirshfeld surfaces [1] and the associated 2D-fingerprint [2] plots were calculated using Crystal Explorer [7] which accepted a structure input file in CIF format. Bond lengths to hydrogen atoms were set to standard values. For each point on the Hirshfeld isosurface, two distances de, the distance from the point to the nearest nucleus external to the surface and di, the distance to the nearest nucleus internal to the surface, were defined. The normalized contact distance (d_{norm}) based on de and di was given by

$$d_{norm} = \frac{(d_i - r_i^{vdw})}{r_i^{vdw}} + \frac{(d_e - r_e^{vdw})}{r_e^{vdw}}$$

where r_i^{vdw} and r_e^{vdw} were the van der Waals radii of the atoms. The value of d_{norm} was negative or positive depending on intermolecular contacts, being shorter or longer than the van der Waals separations. The parameter d_{norm} displayed a surface with a red-white-blue colour scheme, where bright red spots highlighted shorter contacts, white areas represented contacts around the van der Waals separation, and blue regions were devoid of close contacts. For a given crystal structure and set of spherical atomic electron densities, the Hirshfeld surface was unique [8] and it was this property that suggested the possibility of gaining additional insight into the intermolecular interaction of molecular crystals.

The Hirshfeld surface of the complex is mapped over d_{norm} (range -0.1 Å to 1.5 Å), shape index and curvedness (Fig.**S1**). Red spots on the Hirshfeld surfaces mapped with d_{norm} denote the dominant interactions (Fig. **S1**). The main interaction observed for the complex is between nitrogen and hydrogen atoms. Other visible spots in Hirshfeld surfaces correspond to C···H and H···H contacts. The intermolecular interactions appear as distinct spikes in the 2D fingerprint plot (Fig. **S2**).

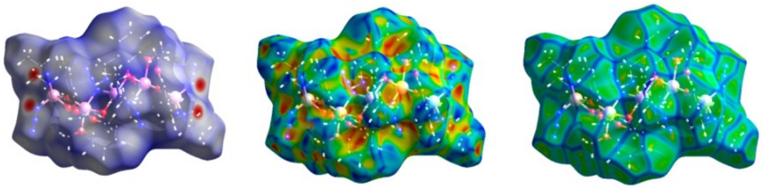

Fig. S1: Hirshfeld surfaces of the complex mapped with d_{norm} (left), shape index (middle) and curvedness (right).

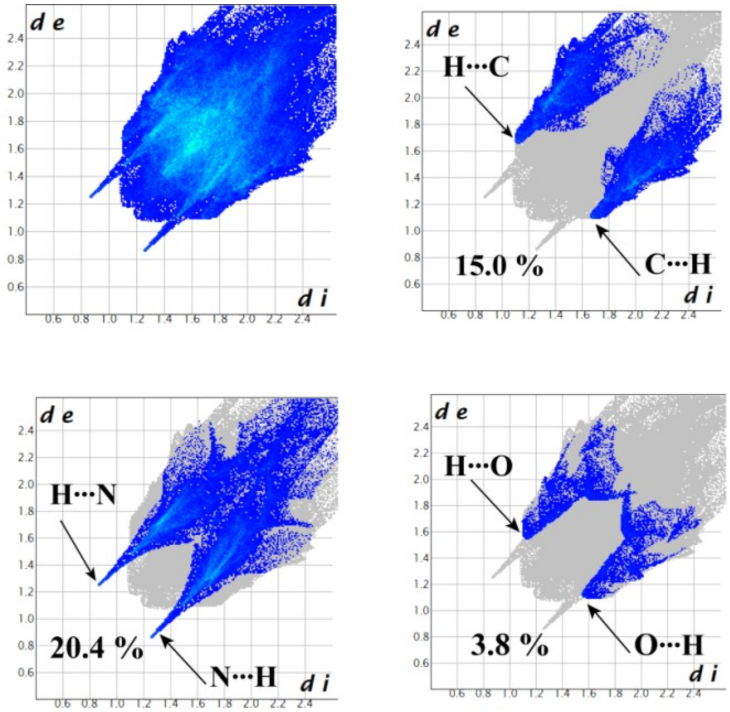

Fig. S2: The proportion of N···H/H···N interactions comprise 20.4% of the Hirshfeld surfaces and the proportion of O···H/H···O and C···H/H···C interactions comprise 3.8% and 15.0% of the Hirshfeld surfaces, respectively.

Reference

1 (a) M.A. Spackman, D. Jayatilaka, CrystEngComm 11 (2009) 19; (b) F.L. Hirshfeld, *Theor. Chim. Acta*, 1977, **44**, 129; (c) H.F. Clausen, M.S. Chevallier, M.A. Spackman, B.B. Iversen, *New J. Chem.*, 2010, **34**, 193.

2 (a) A.L. Rohl, M. Moret, W. Kaminsky, K. Claborn, J.J. McKinnon, B. Kahr, *Cryst. Growth Des.*, 2008, **8**, 4517; (b) A. Parkin, G. Barr, W. Dong, C.J. Gilmore, D. Jayatilaka, J.J. McKinnon, M.A. Spackman, C. C. Wilson, *CrystEngComm*, 2007, **9**, 648; (c) M.A. Spackman, J.J. McKinnon, *CrystEngComm*, 2002, **4**, 378.

3 S.K. Wolff, D.J. Grimwood, J.J. McKinnon, D. Jayatilaka, M.A. Spackman, Crystal Explorer2.0; University of Western Australia: Perth, Australia, 2007, http://hirshfeldsurfacenet.blogspot.com.

4 J.J. McKinnon, M.A. Spackman, A.S. Mitchell, *Acta Cryst.*, 2004, B60, 627.

IR plot of the complex

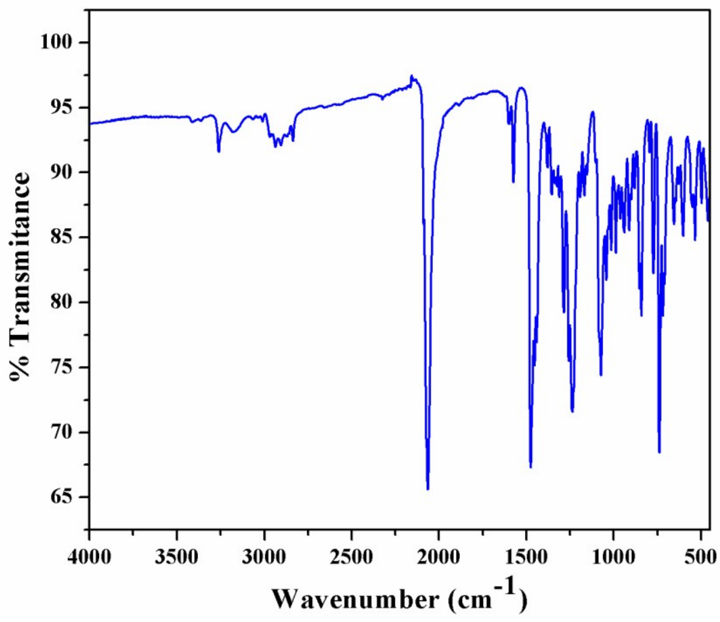

Fig. S3: IR spectrum of the complex**.**

Fluorescence lifetime

Details of the luminescence data of the complex is listed in Table **S1**. Luminescence decay profile of the complex is shown in Fig. **S4**. Intensity decay profile is fitted to the sum of the exponential series;

$$I(t)=\sum_{i} \alpha_i \exp \frac{-t}{\tau_i} \qquad \text{Eq. (1)}$$

where, α_i and τ_{av} are the pre-exponential factor and excited-state luminescence decay time associated with the i-th component, respectively. Bi-exponential series is employed to fit the decay profile of the complex, with obtaining χ2 close to 1. The intensity-averaged life time (τ_{av}) is determined using the following equation:

$$\tau_{av} = \frac{\sum \alpha_i \tau_i^2}{\sum \alpha_i \tau_i} \qquad \text{Eq. (2)}$$

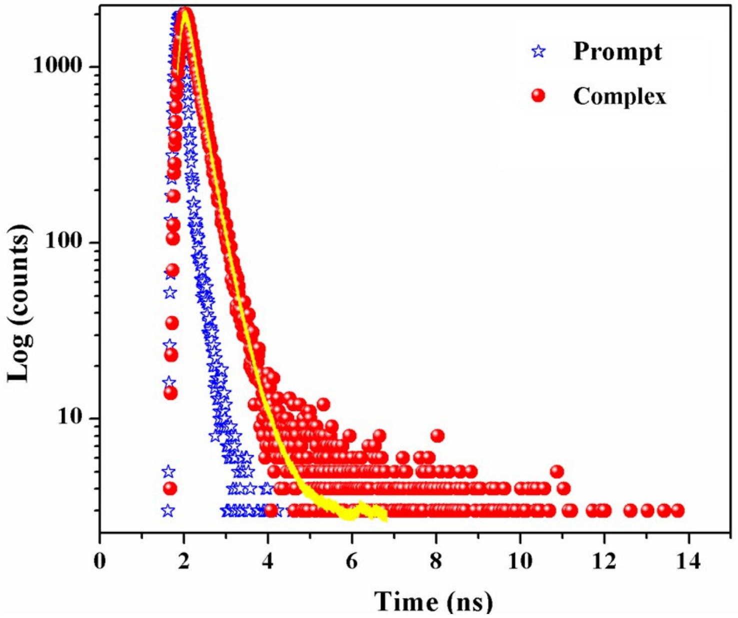

Fig. S4: Fluorescence decay profile of complex.

Table S1: The data of photoluminescence decays of the complex.

λ_{ex} (nm)	λ_{em} (nm)	τ (ns)	χ^2
228	332	55.47	1.1342

Powder X-ray diffraction

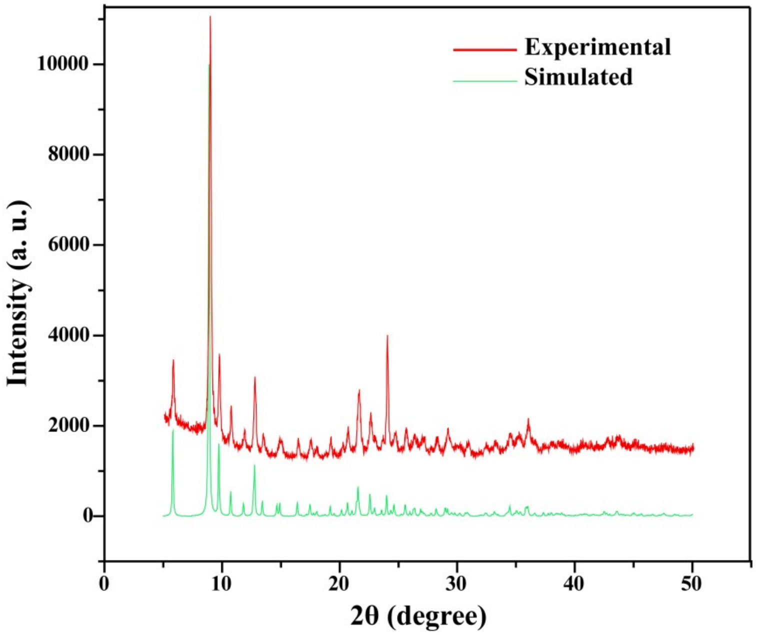

Fig. S5: Experimental and simulated powder XRD patterns of the complex confirming the purity of the bulk materials.

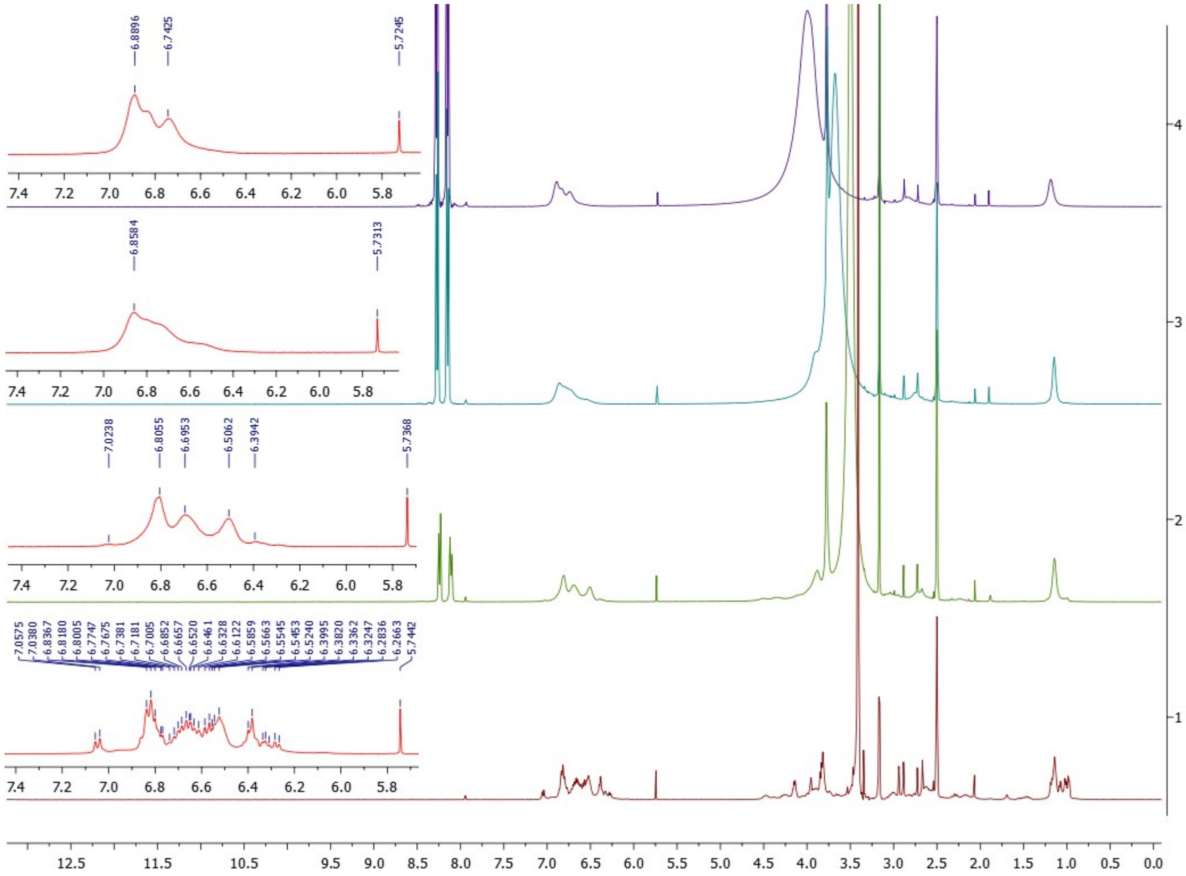

Fig. S6: ^{1}H NMR titration of the complex with varying amounts of 4-nitrobenzoic acid in DMSO-d^6.

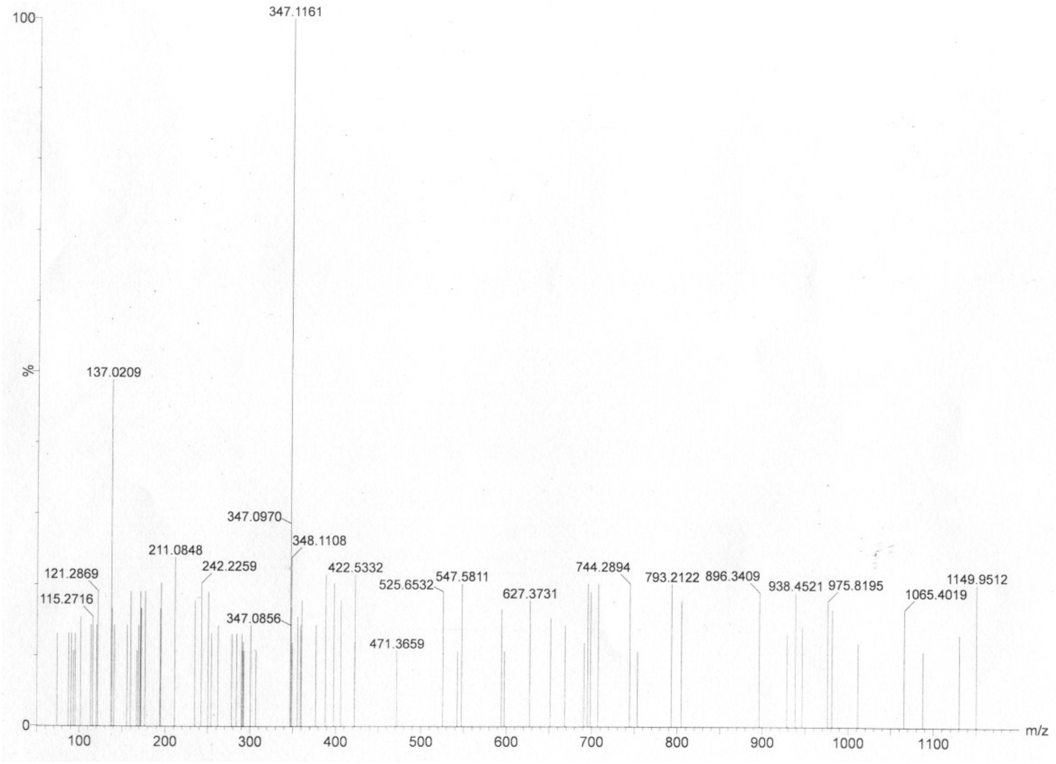

Fig. S7: Mass spectrum of complex with 3-methyl-4-nitrobenzoi acid in DMF.